Korean J. Chem. Eng., 39(11), 3039-3047 (2022)
DOI: 10.1007/s11814-022-1204-2

pISSN: 0256-1115
eISSN: 1975-7220

Selective absorption of H_2S and CO_2 from simulated coke oven gas by aqueous blends of N-methyldiethanolamine and tetramethylammonium glycine

Pan Zhang*, Yuetong Zhao*, Xiangfeng Tian*,, Yanxi Ji*, Yuxuan Shu*, Kun Fu*, Dong Fu*, and Lemeng Wang*,†**

*Hebei Key Lab of Power Plant Flue Gas Multi-Pollutants Control, Department of Environmental Science and Engineering, North China Electric Power University, Baoding, 071003, P. R. China
**Longyuan (Beijing) Carbon Assets Management Technology Co., Ltd. Peking, 100037, P. R. China
(*Received 20 December 2021 • Revised 20 May 2022 • Accepted 10 June 2022*)

Abstract−Tetramethylammonium glycine ($[N_{1111}][Gly]$) can be completely ionized into cation $[N_{1111}]^+$ and anion $[Gly]^-$ in aqueous solution. The anion contains an amino -NH_2 and a carboxyl -COO^-, both of which can react with hydrogen sulfide (H_2S). Therefore, $[N_{1111}][Gly]$ was used to promote the selective absorption of H_2S in coke oven gas (COG) by N-methyldiethanolamine (MDEA). The absorption performance and selectivity of H_2S in the aqueous solution of MDEA-$[N_{1111}][Gly]$ were investigated. The effects of MDEA mass fraction, $[N_{1111}][Gly]$ mass fraction, temperature, H_2S partial pressure and CO_2 partial pressure on the absorption capacity and selectivity were clarified. The results showed that an aqueous solution of MDEA-$[N_{1111}][Gly]$ has good selectivity for H_2S in COG. The absorption capacity was large and the mass fraction of the solute in the absorbent reached more than 0.55, thereby having outstanding advantages in the aspects of saving energy consumption and operating cost and having a good application potential.

Keyworks: COG, H_2S, MDEA-$[N_{1111}][Gly]$, Absorption Capacity, Absorption Selectivity

INTRODUCTION

The coke industry is the basic industry connecting coal and steel production, and plays an important role in the economy. In 2019, China's coke output reached 471 million tons, and the by-product coke oven gas (COG) exceeded 180 billion cubic meters [1]. The comprehensive utilization of a large number of COGs has become a major issue of concern in the coking industry. The efficient removal of hydrogen sulfide (H_2S) in COG is of great significance to improve gas quality, reduce equipment corrosion, reduce environmental pollution and improve the quality of downstream products.

The wet process is often used to remove H_2S in large coking enterprises [2-4]. Absorption processes such as ammonia-sulfur cycle washing [5], vacuum carbonate process [6] and monoethanolamine (MEA) process [7], as well as catalytic oxidation process with Na_2CO_3 and NH_3 as absorbents [8] have been widely used in China. Among them, the MEA approach has attracted wide attention [9-11]. However, the MEA approach still have some disadvantages: (1) The acid corrosion of equipment is strong after desulfurization, the mass fraction of MEA in absorbent is generally not more than 30%, and about 70% of solvent water consumes a great deal of useless work in the process of rich solution regeneration and lean solution cooling, resulting in high operating cost and overall cost; (2) The selectivity of MEA to H_2S and CO_2 is not strong, and the CO_2 content will affect the desulfurization efficiency, especially when the CO_2 volume fraction reaches 3% [12]. Those shortcomings have become the main bottleneck restricting the further popularization and application of MEA desulfurization process.

To reduce the operation cost and improve the selectivity, the blended amine aqueous solution can be used as the absorbent. Li et al. [13] compared the performance of a single MEA and N-methyldiethanolamine (MDEA) aqueous solution with MEA and MDEA mixed aqueous solution in absorbing H_2S, and found that the load of H_2S in blended solution was higher than that in a single solution. An et al. [14] studied the absorption of H_2S by adding diethylenetriamine (DETA) and MEA amine solution to MDEA solution. They found that the addition of MEA and DETA could increase the absorption load and absorption rate of H_2S. Glasscock et al. [15] studied the process of simultaneous removal of H_2S and CO_2 by the mixed solution of MDEA and diethanolamine (DEA), and found that the mixed solution has a good selective removal performance for H_2S. Most studies have shown that the H_2S absorption performance of mixed alkanolamine is better than that of single MEA solution, especially those mixed with MDEA [16-19], because MDEA has many advantages, such as high selectivity, large absorption capacity, low volatility, difficult degradation, low regeneration energy consumption and low corrosivity [20,21]. In addition, when the total mass fraction of the MDEA and the accelerator in the solution is more than 50%, not only can higher selectivity, higher absorption rate and larger absorption quantity be ensured, but also the acid corrosion to equipment can be reduced. At the same time, due to the large reduction of solvent water, the energy consumption of rich solution regeneration and lean solution cooling can be greatly reduced [12-24].

However, most of these current studies only focused on the desulfurization of high-pressure natural gas and high-pressure COG [25-28]. China still has a large number of coke oven by-product low-pressure COG [3,29], in which CO_2 volume fraction is between 1-

†To whom correspondence should be addressed.
E-mail: wanglm@ncepu.edu.cn

3%, H_2S content is between 4-8 g/m^3 [3,30]; its desulfurization efficiency needs to be improved, but the relevant research is less reported. As a class of green solvents, ionic liquids (ILs) have attracted extensive attention owing to their unique properties, such as thermal stability, a wide liquid range, negligible vapor pressure, and structural designability. These characteristics enable ILs with great potential for acid gas separation [31-33]. Damanafshan et al. [34] presented a comprehensive review of systems consisting of CO_2 solubility in aqueous MDEA+ILs mixtures, and concluded that the addition of ILs to aqueous MDEA significantly enhances the absorption of CO_2. Therefore, the emergence of ILs also offers the opportunity to address the above-mentioned goals. Considerable progress has been made in the application of ILs for the selective absorption of H_2S and CO_2. Barati-Harooni et al. [35] developed computer models and provide accurate predictions for solubility of CO_2 and H_2S in ILs. Huang et al. [36] synthesized a series of phenolic ILs and investigated the selective absorption performance of H_2S and CO_2. The results showed that highly efficient and selective absorption of H_2S from CO_2 is realized in phenolic ILs by cooperatively making use of the anionic strong basicity and cationic hydrogen-bond donation. They also found that high H_2S/CO_2, H_2S/CH_4 and CO_2/CH_4 selectivity can be achieved by adjusting the ratio of choline chloride (ChCl) and urea in mixtures [37]. Our previous works [22-24] showed that the blended solution of amino acid ionic liquids (AAILs) with MDEA showed a higher absorption performance of H_2S than that of MDEA-MEA aqueous solution and could meet the II-III level (H_2S≤0.5 g/m^3, HJ/T126-2003) or I level (H_2S≤0.2 g/m^3) of China Cleaner Production Standard. ILs have strong hydrogen bond networks, each H_2S molecule has two hydrogen bond donors and two hydrogen bond acceptor sites, which makes the affinity of ILs with H_2S higher than with CO_2 [38,39]. Seyedhosseini et al. [40] used density functional theory calculations to compare the adsorption performance and selectivity of AAILs for H_2S and CO_2. The results show that the adsorption sites for H_2S contained in the anions of AAILs are twice as much as the adsorption sites for CO_2. The adsorption enthalpy change of the carboxylic groups of AAILs to H_2S is also twice that of CO_2, which confirms that the adsorption selectivity of AAILs to H_2S is higher than that of CO_2. Tetramethylammonium glycine ([N_{1111}][Gly]), which is composed of tetramethylammonium cation and glycine anion, has been proven to have a significant role in promoting the absorption of acid gases [41-43]. It can be completely ionized into a cation $[N_{1111}]^+$ and an anion $[Gly]^-$ in solution, and the anion contains an amino group -NH_2 and a carboxyl group -COO^-, both of which can react with H_2S [40,44]. Thus, it can be used as an accelerator for absorbing H_2S in MDEA aqueous solution. However, absorption performance and selectivity of low partial pressure H_2S and CO_2 in COG have not been well documented.

Focused on the issue of H_2S removal from COG, the main purpose of this work is to (1) promote the absorption performance of MDEA absorbent using [N_{1111}][Gly], and then establish a lean water absorption system; (2) experimentally determine the absorption capacity and absorption selectivity; (3) elucidate the influence factors and rules of absorption capacity and absorption selectivity.

EXPERIMENTAL SECTION

1. Materials and Apparatus

The absorbent is [N_{1111}][Gly] promoted MDEA aqueous solution. The simulated gas consists of H_2S, CO_2 and N_2. Sample information is shown in Table 1. Taking purity into account, the uncertainties of w_{MDEA} and $w_{[N1111][Gly]}$ are, respectively, estimated as 0.010 and 0.005. The apparatus used in the experiment is shown in Table 2. The measuring range of the electronic analytical balance is 0-160 g, and the uncertainty is ±0.1 mg. The H_2S analyzer measures the H_2S concentration by the three-electrode potentiostat method, the measurement range is 0-5,000 ppm, and the uncertainty is ±2% F.S. The measurement principle of the CO_2 analyzer is non-dispersive infrared NDIR, the measurement range is 0-20 vol%, and the uncertainty is ±2% F. S.

The stirring speed of the magnetic stirrer ranges from 0 to 6,000 rpm, the controllable temperature range of the thermostatic water bath is 273.2 K-373.2 K, and the uncertainty is ±0.1 K. The mass flow controller can control the gas flow in the range of 0-200 mL/min, and the uncertainty is ±0.5% F. S. The experimental pipelines were connected by PTFE pipes and kept at a certain temperature by temperature-controlled heating strips.

2. Procedure

The absorption equipment, shown in Fig. 1, mainly includes mixed gas supply, H_2S and CO_2 absorption, tail gas analysis and data recording, and tail gas treatment. Because of the toxicity of H_2S, before the start of the experiment, N_2 was introduced and the gas tightness of the whole experimental pipeline was checked with soapy water. During the experiment, N_2, CO_2 and H_2S in the high pressure cylinder were reduced to 1 atm, respectively, by the pressure reducing valve, and the flow rates of H_2S, CO_2 and N_2 (v_{H_2S}, v_{CO_2} and

Table 1. Sample description

Chemical name	CAS	Purity (mole fraction, as stated by the supplier)	Source
MDEA	105-59-9	≥0.98	Aladdin Reagent
[N_{1111}][Gly]	158474-94-3	≥0.99	Shanghai Cheng Jie Chemical Co., Ltd
H_2S	7783-06-4	0.0999	Baoding Hanjiangxue Trading Company
CO_2	124-38-9	≥0.9999	Baoding Hanjiangxue Trading Company
N_2	7727-37-9	≥0.9999	Baoding Hanjiangxue Trading Company
H_2O	7732-18-5	Electrical resistivity>15 MΩ·cm at T=298 K	Heal force ROE-100 apparatus

Table 2. Experimental apparatus

Experimental instrument	Model	Relative uncertainty	Manufacturer (Co. Ltd.)
Analytical balance	FA1604A	±0.1 mg	Shanghai Jingtian Electronic Instrument
H_2S analyzer	CGM10-70	±2% F.S.	Shenzhen Angwei Electronic
CO_2 analyzer	AGM DTME III	±2% F.S.	Shenzhen Angwei Electronic
Vacuum drying oven	DZF-6050	±0.1 K	Shanghai Xinmiao Medical Apparatus Manufacturing
Constant temperature heating magnetic stirrer	DF-101S	±0.1 K	Gongyi Yuhua Instrument
Mass flow controllers (MFC)	CS200A	±0.5% F. S.	Beijing Sevenstar Huachuang Electronic
Constant temperature water bath	HWY-501	±0.1 K	Shanghai Changji Geological Instrument

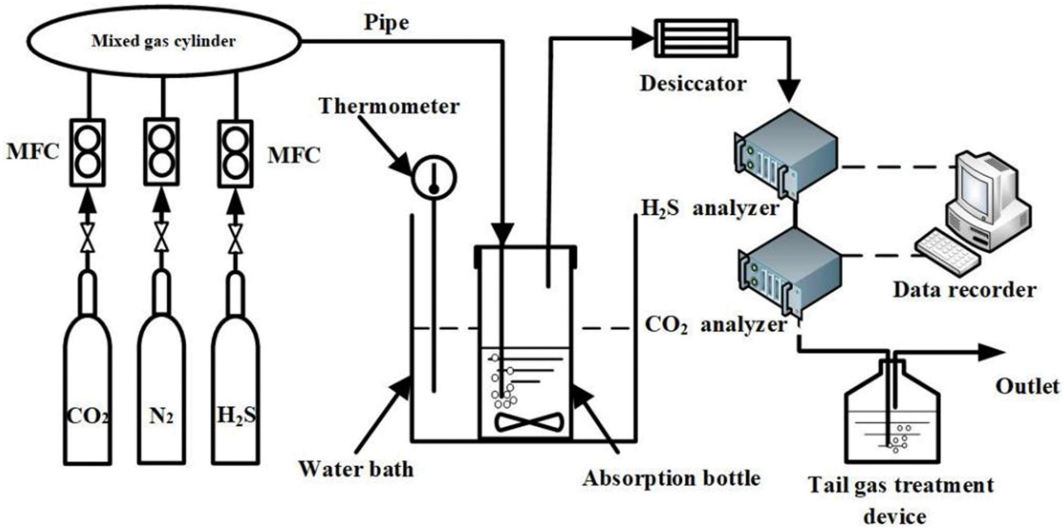

Fig. 1. Schematic diagram for H_2S absorption.

v_{N_2}) were controlled by three MFCs to keep constant, and the total flow rate was maintained at 400 mL/min. The three gases enter a gas mixing cylinder to be evenly mixed and then enter a gas absorption device.

The prepared absorbent is put into a water bath for preheating. After the concentration of H_2S and CO_2 in the analyzers reaches the set value and kept constant for one hour, the absorbent is poured into the absorption bottle. At the same time, experimental data is recorded. After the reactor, the gas goes to a condenser and then is dried by anhydrous calcium chloride. During the experiment, the concentration of H_2S and CO_2 in the tail gas will first decrease rapidly, and then increase slowly. When the indicator in the H_2S analyzer reaches the set value again, it is considered that the absorption of H_2S by the absorbent reaches saturation. At this time, the absorbent may not be saturated with CO_2, but since H_2S is the main impurity to be removed, the experiment can be terminated.

Finally, the H_2S and CO_2 not absorbed in the tail gas are absorbed by the NaOH solution and discharged outdoors through the exhaust hood. The total volume of H_2S and CO_2 absorbed by the absorbent is calculated by the following formula:

$$V_{H_2S} = v_{H_2S}t - \sum_{i=0}^{t}\left(c_{H_2S,\,i} \times \frac{v(1 - c_{H_2S,\,0} - c_{CO_2,\,0})}{1 - c_{H_2S,\,i} - c_{CO_2,\,i}} \times \Delta t\right) \quad (1)$$

$$V_{CO_2} = v_{CO_2}t - \sum_{i=0}^{t}\left(c_{CO_2,\,i} \times \frac{v(1 - c_{H_2S,\,0} - c_{CO_2,\,0})}{1 - c_{H_2S,\,i} - c_{CO_2,\,i}} \times \Delta t\right) \quad (2)$$

in which V_{H_2S} and V_{CO_2} are the absorbed volumes of H_2S and CO_2 (mL), v_{H_2S} and v_{CO_2} are the initial flow rates of H_2S and CO_2 (mL/min), v is the total flow rate of the gas mixture. $c_{H_2S,0}$ and $c_{CO_2,0}$ are the volume fractions of H_2S and CO_2, $c_{H_2S,i}$ and $c_{CO_2,i}$ are the volume fractions of H_2S and CO_2 at time i (s). t is the absorption time (s). Δt in Eqs. (1) and (2) is set as 1 s.

The absorption amount of H_2S and CO_2 can be calculated from:

$$m_{H_2S} = \frac{273.15}{T} \times \frac{V_{H_2S}/1{,}000}{22.4} \times \frac{34.08}{M} \quad (3)$$

$$m_{CO_2} = \frac{273.15}{T} \times \frac{V_{CO_2}/1{,}000}{22.4} \times \frac{44}{M} \quad (4)$$

in which T and M are temperature (K) and mass of absorbent (g), respectively. The accuracy of the experimental equipment was ver-

ified in our previous research [22-24].

Selectivity of H_2S and CO_2 (S_{H_2S/CO_2}) can be calculated from [45, 46]:

$$S_{H_2S/CO_2}=\frac{(n_{H_2S}/n_{CO_2})_L}{(n_{H_2S}/n_{CO_2})_g} \quad (5)$$

in which n_{H_2S} and n_{CO_2} are moles of H_2S and CO_2, L and g stand for liquid phase and gas phase, respectively.

RESULTS AND DISCUSSION

1. Reaction Principle

The reaction between H_2S and MDEA is a proton transfer reaction, and the rate constant is more than 10^9 L/(mol·s), so it can be considered that the reaction is instantaneous [46]. MDEA does not react with CO_2 under anhydrous conditions. The reaction rate of MDEA with H_2S is much higher than that of MDEA with CO_2, which provides convenience for the selective removal of H_2S.

$$H_2S+RR'_2N \rightleftharpoons HS^-+RR'_2NH^+ \quad (R\text{-}1)$$

in which R=CH_3, R′=$OHCH_2CH_2$.

$$CO_2+H_2O \rightleftharpoons H^++HCO_3^- \quad (R\text{-}2)$$

$$H^++RR'_2N \rightleftharpoons RR'_2NH^+ \quad (R\text{-}3)$$

$$CO_2+H_2O+RR'_2N \rightleftharpoons HCO_3^-+RR'_2NH^+ \quad (R\text{-}4)$$

$$[N_{1111}][Gly] \rightarrow [N_{1111}]^++H_2N\text{-}CH_2\text{-}COO^- \quad (R\text{-}5)$$

$$R''NH_2^-+H_2S \rightleftharpoons R''NH_3+HS^- \quad (R\text{-}6)$$

$$R'''COO^-+H_2S \rightleftharpoons R'''COOH+HS^- \quad (R\text{-}7)$$

in which R″=-CH_2-COO^-, represents the moiety of the anion $[Gly]^-$ other than the amino group, and R‴=-CH_2-NH_2, represents the moiety of the anion $[Gly]^-$ other than the carboxyl group.

The reaction mechanism is shown in Fig. 2. First, H_2S and CO_2 dissolved in water to form H^+. After that, the H^+ was transferred to MDEA and $[Gly]^-$, respectively. For MDEA, the product is carbamate, but for $[Gly]^-$, the products are different. The $[N_{1111}][Gly]$ selected in this work contains carboxyl and multiple amino groups, which can provide active sites for the absorption of H_2S. The two H atoms in H_2S molecule can combine with the N and O atoms in these two groups to form -S-H···N bond and -S-H···O bond, while the presence of carboxyl group will inhibit the dissolution of CO_2 to a certain extent [39,40], thus providing convenience for the selective removal of H_2S. In summary, the mechanism of H_2S and CO_2 capture in MDEA-$[N_{1111}][Gly]$ aqueous solution was the competition for protons.

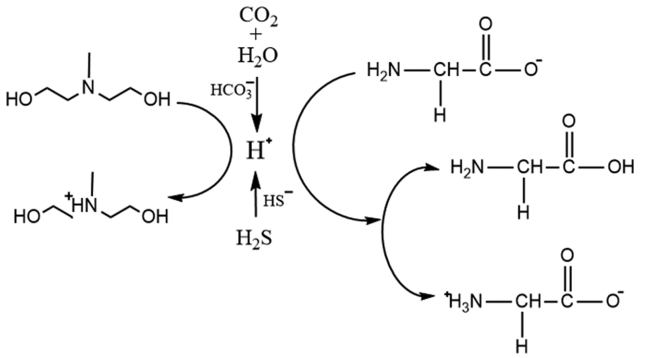

Fig. 2. Mechanism of H_2S and CO_2 capture in MDEA-$[N_{1111}][Gly]$ aqueous solution.

2. Absorption Capacity and Selectivity

The mass fraction of the absorbent solute was set as 32.5% to 57.5%, in which the mass fraction of the accelerator varied from 2.5% to 7.5%. The main reason is that adding a small amount of accelerator can achieve the effect of promotion. The H_2S partial pressure was set between 300 Pa and 500 Pa, and the volume concentration of CO_2 was between 1% and 3%. The temperature ranged from 303.2 K to 323.2 K, and the results are shown in Tables 3-5.

In general, it is known that the S_{H_2S/CO_2} and absorption capacity and according to the change of the operation variable changes. In the above three tables, the range of each factor was set to be relatively wide to obtain the influence of operating conditions on the S_{H_2S/CO_2} and absorption capacity of H_2S and CO_2. The selectivity in-

Table 3. Absorption capacity (m) of H_2S and CO_2 in MDEA-$[N_{1111}][Gly]$ aqueous solutions and the corresponding selectivity factor under different CO_2 pressure. p_{H_2S}=500 Pa, T=313.2 K[a]

w_{MDEA}	$w_{[N1111][Gly]}$	m/(g H_2S per 100 g aqueous solution)			m/(g CO_2 per 100 g aqueous solution)			Selectivity factor		
		1 vol%	2 vol%	3 vol%	1 vol%	2 vol%	3 vol%	1 vol%	2 vol%	3 vol%
0.300	0.025	0.581	0.509	0.436	1.305	1.847	2.090	1.15	1.42	1.62
	0.050	0.645	0.564	0.469	1.420	2.011	2.216	1.17	1.45	1.64
	0.075	0.711	0.631	0.517	1.535	2.203	2.399	1.20	1.48	1.67
0.400	0.025	0.616	0.533	0.469	1.080	1.616	1.950	1.47	1.70	1.86
	0.050	0.677	0.591	0.509	1.171	1.772	2.102	1.49	1.72	1.88
	0.075	0.742	0.666	0.558	1.260	1.969	2.278	1.52	1.75	1.90
0.500	0.025	0.605	0.518	0.455	0.925	1.285	1.559	1.69	2.08	2.26
	0.050	0.667	0.587	0.489	1.008	1.432	1.662	1.71	2.12	2.28
	0.075	0.673	0.655	0.532	1.131	1.563	2.090	1.72	2.16	2.30

[a]Expanded uncertainties U at a 95% confidence level are U_{95} (T)=0.1 K; $U_{r,95}$ (p)=2%; U_{95} (w_{MDEA})=0.010; U_{95} ($w_{[N1111][Gly]}$)=0.005; $U_{r,95}$ (m)=1.6%.

Table 4. Absorption capacity (m) of H_2S and CO_2 in MDEA-[N_{1111}][Gly] aqueous solutions and the corresponding selectivity factor under different H_2S pressure. CO_2=2 vol%, T=313.2 K[a]

w_{MDEA}	$w_{[N1111][Gly]}$	m/(g H_2S per 100 g aqueous solution)			m/(g CO_2 per 100 g aqueous solution)			Selectivity factor		
		300 Pa	400 Pa	500 Pa	300 Pa	400 Pa	500 Pa	300 Pa	400 Pa	500 Pa
0.300	0.025	0.307	0.411	0.509	1.937	1.905	1.847	1.36	1.39	1.42
	0.050	0.354	0.468	0.564	2.215	2.113	2.011	1.38	1.43	1.45
	0.075	0.408	0.518	0.631	2.485	2.309	2.203	1.41	1.45	1.48
0.400	0.025	0.324	0.423	0.533	1.721	1.647	1.616	1.62	1.66	1.70
	0.050	0.359	0.467	0.591	1.895	1.788	1.772	1.63	1.69	1.72
	0.075	0.387	0.522	0.666	2.006	1.952	1.969	1.66	1.73	1.75
0.500	0.025	0.317	0.401	0.518	1.427	1.301	1.285	1.91	1.99	2.08
	0.050	0.352	0.452	0.587	1.565	1.439	1.432	1.94	2.03	2.12
	0.075	0.381	0.487	0.655	1.679	1.543	1.563	1.95	2.04	2.16

[a]Expanded uncertainties U at a 95% confidence level are U_{95} (T)=0.1 K; $U_{r,95}$ (p)=2%; U_{95} (w_{MDEA})=0.010; U_{95} ($w_{[N1111][Gly]}$)=0.005; $U_{r,95}$ (m)=1.6%.

Table 5. Absorption capacity (m) of H_2S and CO_2 in MDEA-[N_{1111}][Gly] aqueous solutions and the corresponding selectivity factor under different temperature. p_{H_2S}=500 Pa, CO_2=2 vol%[a]

w_{MDEA}	$w_{[N1111][Gly]}$	m/(g H_2S per 100 g aqueous solution)			m/(g CO_2 per 100 g aqueous solution)			Selectivity factor		
		303.2 K	313.2 K	323.2 K	303.2 K	313.2 K	323.2 K	303.2 K	313.2 K	323.2 K
0.300	0.025	0.579	0.509	0.379	1.983	1.847	1.717	1.51	1.42	1.14
	0.050	0.628	0.564	0.434	2.114	2.011	1.881	1.53	1.45	1.19
	0.075	0.691	0.631	0.501	2.289	2.203	2.073	1.56	1.48	1.25
0.400	0.025	0.620	0.533	0.403	1.752	1.616	1.486	1.83	1.70	1.40
	0.050	0.671	0.591	0.461	1.878	1.772	1.642	1.85	1.72	1.45
	0.075	0.719	0.666	0.536	1.975	1.969	1.839	1.88	1.75	1.51
0.500	0.025	0.626	0.518	0.388	1.421	1.285	1.155	2.28	2.08	1.73
	0.050	0.676	0.587	0.457	1.518	1.432	1.302	2.30	2.12	1.81
	0.075	0.731	0.655	0.509	1.609	1.563	1.433	2.35	2.16	1.83

[a]Expanded uncertainties U at a 95% confidence level are U_{95} (T)=0.1 K; $U_{r,95}$ (p)=2%; U_{95} (w_{MDEA})=0.010; U_{95} ($w_{[N1111][Gly]}$)=0.005; $U_{r,95}$ (m)=1.6%.

creased with increasing temperature, w_{MDEA} and CO_2 volume fraction. 20 K, 20 wt% and 2 vol% increases in temperature, w_{MDEA} and CO_2 mole fraction caused about 20%, 30% and 40% increase in selectivity, respectively. The influence of the mole fraction of [N_{1111}][Gly] and H_2S partial pressure on the selectivity showed a very slight increase. Jalili et al. [47] demonstrated that S_{H_2S/CO_2} in [C_8mim][Tf_2N] ranges from 2.8-3.1 at 303.2 K and 0.1 MPa and S_{H_2S/CO_2} in [C_2mim][eFAP] shows a very slight decrease from 1.82 to 1.78 when the CO_2 mole fraction increases from 0.2 to 0.8 at 303.15 K and 0.1 MPa [48]. Shiflett et al. [49] found that S_{H_2S/CO_2} in [Bmin][$MeSO_4$] aqueous solution decreases from about 13.5 to about 7.5 as the CO_2/H_2S mole ratio decreases from 4 : 1 to 1 : 4 at 303.15 K and 0.1 MPa. Huang et al. [50] found that S_{H_2S/CO_2} in four protic ILs ([MDEAH][Ac], [MDEAH][For], [DMEAH][Ac] and [DMEAH][For]) ranges from 8.9-19.5 at 303.2 K, almost a magnitude larger than that in normal ILs, and [TMGH][PhO] with high selectivity of H_2S/CO_2 (6.2 at 313.2 K and 0.1 bar) was also found [36]. A comparison with these previous results shows that MDEA-[N1111][Gly] is less effective for the separation of CO_2 and H_2S gases from each other in gaseous streams. Also, the result shows that MDEA-[N1111][Gly] aqueous solution can remove these two acid gases from COG effectively.

2-1. Effect of CO_2 Concentration

The CO_2 concentration dependence of absorption capacity of H_2S and CO_2 and S_{H_2S/CO_2} in MDEA-[N_{1111}][Gly] aqueous solutions is shown in Fig. 3 at 313.2 K and 0.1 MPa. The absorption capacity of H_2S and CO_2 decreases and increases with the increasing CO_2 concentration in Fig. 3(a), respectively. The S_{H_2S/CO_2} increases by increasing CO_2 concentration. Such a phenomenon indicates that there is a competitive relationship between H_2S and CO_2 in the absorption process. Moreover, since the partial pressure of CO_2 in the mixed gas is much higher than that of H_2S, the absorption capacity of MDEA-[N_{1111}][Gly] aqueous solutions to CO_2 is larger than that to H_2S.

2-2. Effect of H_2S Concentration

When the partial pressure of H_2S changes from 300 Pa to 500

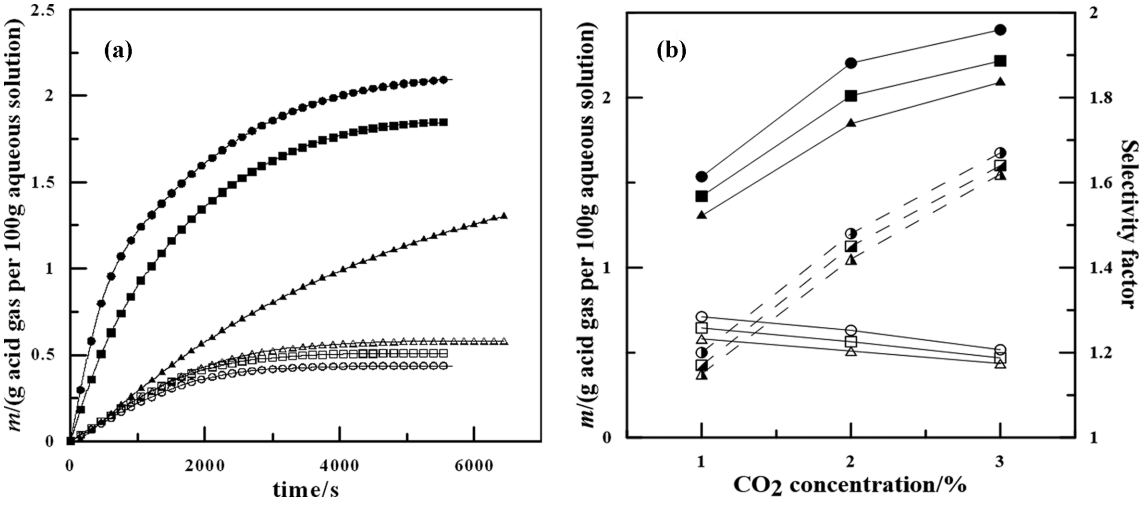

Fig. 3. Effect of CO_2 concentration on absorption capacity of H_2S (△□○) and CO_2 (▲■●) and H_2S/CO_2 selectivity (◭◪◑), (a) w_{MDEA}= 0.300; $w_{[N1111][Gly]}$=0.025; T=313.2 K; p_{H_2S}=500 Pa; △▲CO_2=1 vol%; □■CO_2=2 vol%; ○●CO_2=3 vol%; (b) w_{MDEA}=0.300; T=313.2 K; p_{H_2S}=500 Pa; △▲◭$w_{[N1111][Gly]}$=0.025; □■◪$w_{[N1111][Gly]}$=0.050; ○●◑$w_{[N1111][Gly]}$=0.075; Lines: trend values.

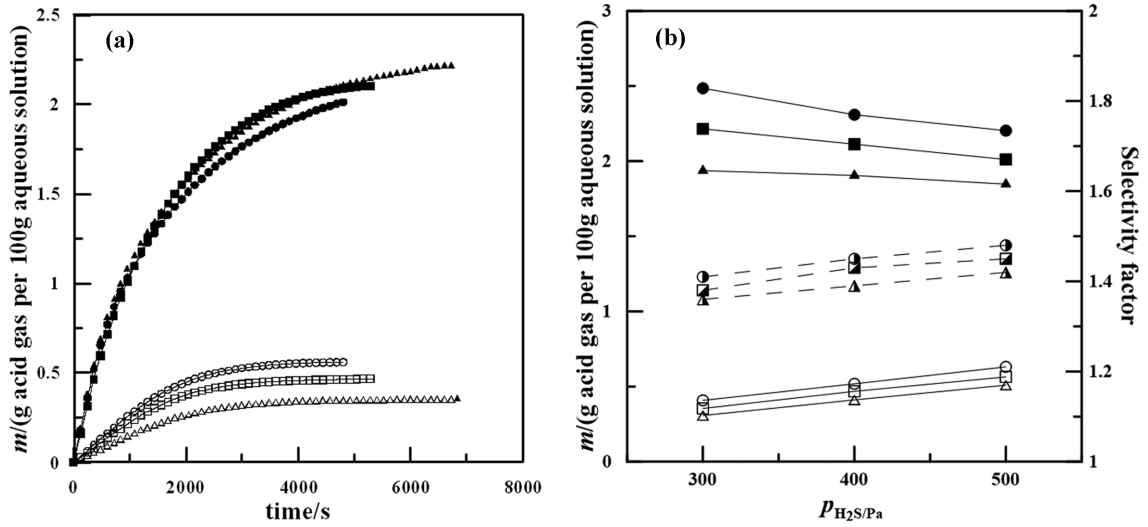

Fig. 4. Effect of H_2S concentration on absorption capacity of H_2S (△□○) and CO_2 (▲■●) and H_2S/CO_2 selectivity (◭◪◑), (a) w_{MDEA}/ $w_{[N1111][Gly]}$=0.300/0.050; CO_2=2 vol%; T=313.2 K; △▲p_{H_2S}=300 Pa; □■p_{H_2S}=400 Pa; ○●p_{H_2S}=500 Pa; (b) w_{MDEA}=0.300; CO_2=2 vol%; T=313.2 K; △▲◭$w_{[N1111][Gly]}$=0.025; □■◪$w_{[N1111][Gly]}$=0.050; ○●◑$w_{[N1111][Gly]}$=0.075; Lines: trend values.

Pa, the absorption capacity of H_2S and CO_2 and S_{H_2S/CO_2} in MDEA-$[N_{1111}][Gly]$ aqueous solution is shown in Fig. 4. The absorption capacity of H_2S and CO_2 increased and decreased with the increase of H_2S partial pressure, respectively. For example, in the case of $w_{MDEA}/w_{[N1111][Gly]}$=0.300/0.050, when H_2S partial pressure increased from 300 Pa to 500 Pa, the absorption capacity of H_2S increased from 0.354 g to 0.564 g, *i.e.*, a 59.32% increase resulted. The absorption capacity of CO_2 decreased from 1.721 g to 1.616 g, with a 6.10% decrease. In addition, the S_{H_2S/CO_2} remains a relatively slow growth with increasing H_2S concentration, *i.e.*, S_{H_2S/CO_2} enhancement is about 5%. This trend can be observed for all H_2S fractions.

2-3. Effect of Absorbent Concentration

The effect of MDEA concentration on the absorption capacity and selectivity is shown in Fig. 5. It can be seen that the absorption capacity of H_2S remains relatively constant with increasing w_{MDEA}. While the absorption capacity of CO_2 shows a downward trend, and the S_{H_2S/CO_2} shows an upward trend. For example, in the case of T=313.2 K and $w_{[N1111][Gly]}$=0.025 (Fig. 5(a)), when w_{MDEA} increased from 0.300 to 0.500, H_2S absorption capacity increased from 0.509 g to 0.518 g, with a 1.77% increase. CO_2 absorption capacity decreased from 1.847 g to 1.285 g, with a 30.43% decrease. The S_{H_2S/CO_2} increased from 1.42 to 2.08.

The time corresponding to the saturation of H_2S absorption was taken as an experimental period in each experiment. With the increase of MDEA concentration in the absorption solution, the viscosity of the solution increases rapidly, so the absorption rate of CO_2 decreases continuously, the absorption amount of CO_2 decreases gradually in the experimental period, and the selectivity factor in-

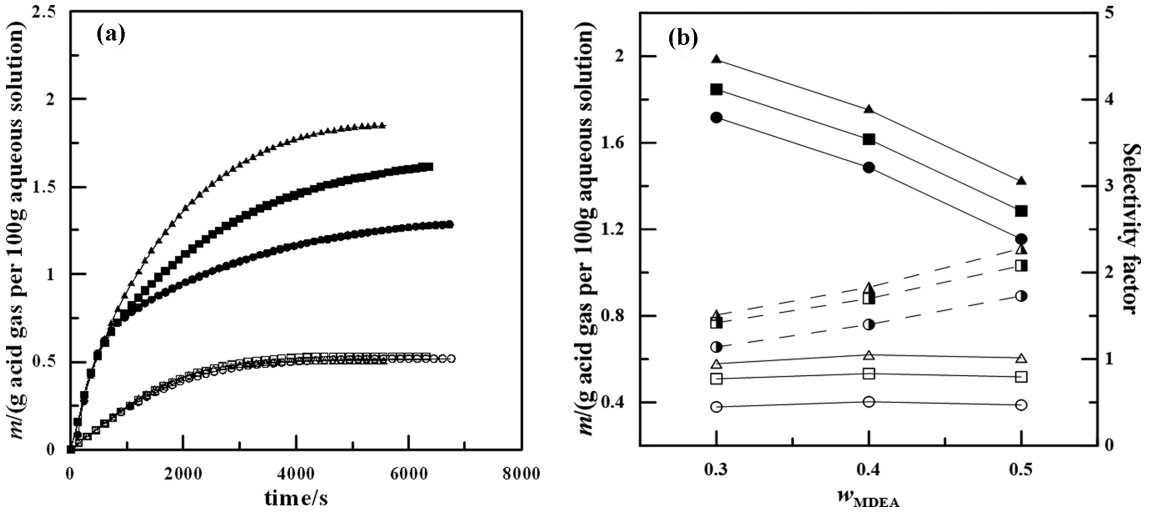

Fig. 5. Effect of w_{MDEA} on absorption capacity of H_2S (△□○) and CO_2 (▲■●) and H_2S/CO_2 selectivity (◭◪◑), (a) $w_{[N1111][Gly]}$=0.025; CO_2=2 vol%; T=313.2 K; p_{H_2S}=500 Pa; △▲w_{MDEA}=0.300; □■w_{MDEA}=0.400; ○●w_{MDEA}=0.500; (b) $w_{[N1111][Gly]}$=0.025; CO_2=2 vol%; p_{H_2S}=500 Pa; △▲◭T=303.2 K; □■◪T=313.2 K; ○●◑T=313.2 K; Lines: trend values.

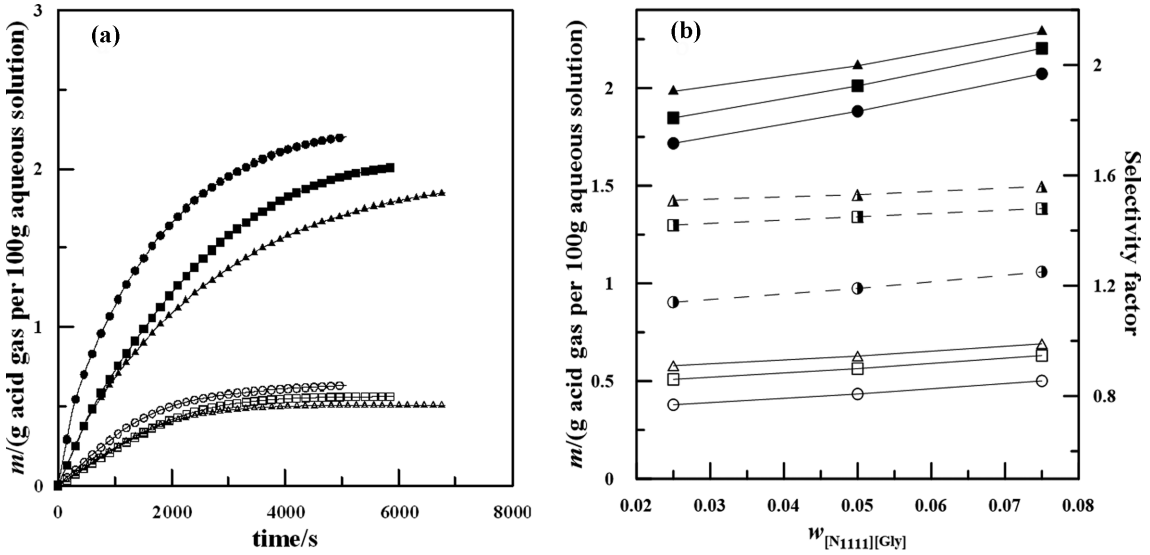

Fig. 6. Effect of $w_{[N1111][Gly]}$ on absorption capacity of H_2S (△□○) and CO_2 (▲■●) and H_2S/CO_2 selectivity (◭◪◑), (a) w_{MDEA}=0.300; CO_2=2 vol%; T=313.2 K; p_{H_2S}=500 Pa; △▲$w_{[N1111][Gly]}$=0.025; □■$w_{[N1111][Gly]}$=0.050; ○●$w_{[N1111][Gly]}$=0.075; (b) w_{MDEA}=0.300; CO_2=2 vol%; p_{H_2S}=500 Pa; △▲◭T=303.2 K; □■◪T=313.2 K; ○●◑T=313.2 K; Lines: trend values.

creases gradually.

The effect of $[N_{1111}][Gly]$ concentration on the absorption capacity and selectivity is shown in Fig. 6. It can be seen that with the increase of $w_{[N1111][Gly]}$, the absorption capacity of H_2S and CO_2 shows an upward trend and the selectivity changes slightly. For example, in the case of T=313.2 K and w_{MDEA}=0.300 (Fig. 6(a)), when $w_{[N1111][Gly]}$ increases from 0.025 to 0.075, the absorption capacity of H_2S increases from 0.509 g to 0.631 g with a 23.96% increase; the absorption capacity of CO_2 increases from 1.847 g to 2.203 g with a 19.27% increase. There is a slight selectivity enhancement.

When $w_{[N1111][Gly]}$ changed from 0.050 to 0.075, the promoting effect became less significant, especially when w_{MDEA} was high. The study of Shiflett and Yokozeki [51] also showed that when CO_2 : H_2S changed from 1 : 9 to 9 : 1 and $w_{[Bmim][PF6]}$ was less than 0.5, the selectivity of H_2S was almost unchanged with the increase of $w_{[Bmim][PF6]}$. The addition of $[N_{1111}][Gly]$ promoted the absorption of the two kinds of acid gases, but the selectivity factor did not change significantly.

2-4. Effect of Temperature

The effect of temperature on the absorption capacity and selectivity is shown in Fig. 7. One finds from this figure that with the increase of temperature, the absorption capacity of H_2S and CO_2 shows a downward trend, and the selectivity gradually decreases. As shown in Fig. 7(b), with increasing temperature from (303.2 to 323.2) K, the H_2S/CO_2 selectivity decreases from 2.30 to 1.81, the absorption capacity of H_2S and CO_2, respectively, decreases from

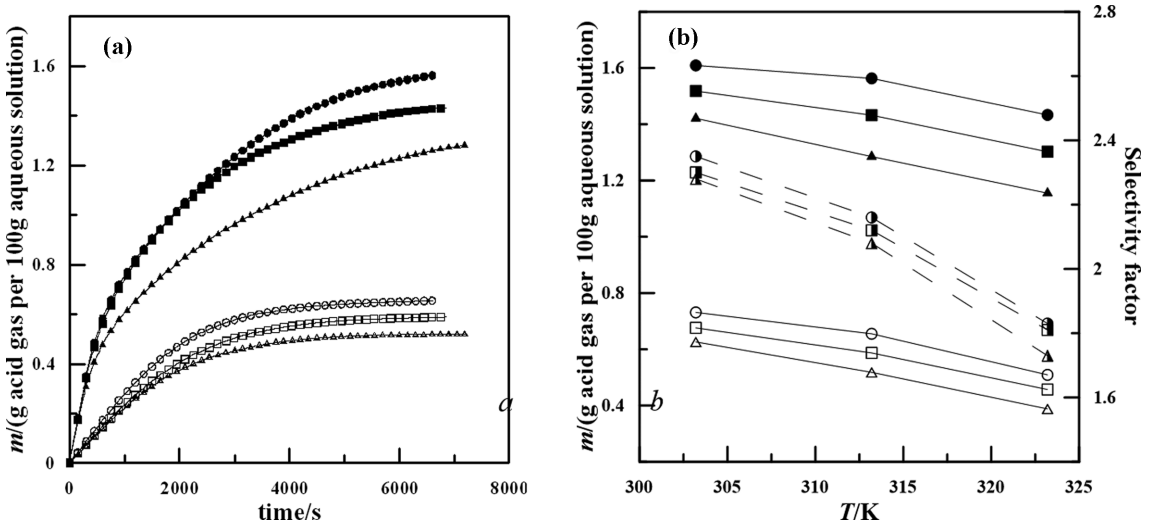

Fig. 7. Effect of temperature on absorption capacity of H_2S (△□○) and CO_2 (▲■●) and H_2S/CO_2 selectivity (◮◪◑), (a) w_{MDEA}/$w_{[N1111][Gly]}$=0.500/0.050; CO_2=2 vol%; p_{H_2S}=500 Pa; △ ▲T=303.2 K; □ ■T=313.2 K; ○ ●T=323.2 K; (b) w_{MDEA}=0.500; CO_2=2 vol%; p_{H_2S}=500 Pa; △ ▲◮$w_{[N1111][Gly]}$=0.025; □ ■◪$w_{[N1111][Gly]}$=0.050; ○ ●◑$w_{[N1111][Gly]}$=0.075; Lines: trend values.

0.676 to 0.457 and 1.518 to 1.302, i.e., a 20 K increase in temperature causes more than 20%, 30% and 10% decrease in H_2S/CO_2 selectivity and absorption capacity of H_2S and CO_2, respectively. The absorption of H_2S and CO_2 is an exothermic process and the increase of temperature results in hindering forward reaction. In addition, the reaction rate constant (k) is a function of temperature and increases with the increasing temperature. Although, the reversibility of the H_2S-amines reaction is more pronounced at higher temperatures. This is why the selectivity showed a tendency to decrease with the increase of temperature. Similar phenomenon can be found in Lu's work [46].

CONCLUSION

The absorption capacity and selectivity of H_2S and CO_2 in MDEA-$[N_{1111}][Gly]$ aqueous solution were measured, and the effects of mass fraction, temperature and partial pressures of H_2S and CO_2 on the absorption capacity and selectivity were clarified. The conclusions are as follows:

(1) With the increase of w_{MDEA}, the absorption capacity of H_2S increased first and then decreased, and the selectivity increased significantly. Higher w_{MDEA} was more conducive to the selective removal of H_2S.

(2) The addition of $[N_{1111}][Gly]$ into MDEA aqueous solution can obviously increase the absorption capacity of H_2S and CO_2. The absorption capacity and selectivity of H_2S and CO_2 decrease with the increase of temperature, and a lower temperature is more beneficial to the selective removal of H_2S.

(3) The increase of H_2S partial pressure can increase the absorption capacity of H_2S, and the existence of CO_2 will hinder the H_2S absorption. The increase of CO_2 partial pressure is beneficial to the improvement of selectivity.

(4) The absorption capacity was large and the mass fraction of the solute in the absorbent reached more than 0.55, thereby having outstanding advantages in the aspects of saving energy consumption and operating cost and having a good application potential.

ACKNOWLEDGEMENTS

This work was supported by the National Natural Science Foundation of China (No. 51776072 and NO. 52106009), the Fundamental Research Funds for the Central Universities (No. 2022MS108) and the Natural Science Foundation of Hebei Province (No. E2021502024 and No.E2020502044).

DECLARATION OF COMPETING INTEREST

The authors declare that they have no known competing financial interests or personal relationships that could have appeared to influence the work reported in this paper.

NOMENCLATURE

$[N_{1111}][Gly]$: tetramethylammonium glycine
H_2S : hydrogen sulfide
COG : coke oven gas
MDEA : N-methyldiethanolamine
MEA : monoethanolamine
DEA : diethanolamine
DETA : diethylenetriamine
AAILs : amino acid ionic liquids
v_{H_2S} : flow rates of H_2S [mL/min]
v_{CO_2} : flow rates of CO_2 [mL/min]
v_{N_2} ; flow rates of N_2 [mL/min]
v : total flow rate of the gas mixture [mL/min]
V_{H_2S} : absorbed volumes of H_2S [mL]
V_{CO_2} : absorbed volumes of CO_2 [mL]
$c_{H_2S,0}$: initial volume fractions of H_2S [%]
$c_{CO_2,0}$: initial volume fractions of CO_2 [%]
$c_{H_2S,i}$: volume fractions of H_2S at time i [%]

$c_{CO_2,i}$: volume fractions of CO_2 at time i [%]
T : temperature [K]
P_{H_2S} : partial pressure of H_2S [Pa]
n_{H_2S} : moles of H_2S
n_{CO_2} : moles of CO_2
t : absorption time
m_{H_2S} : absorption amount of H_2S
m_{CO_2} : absorption amount of CO_2
w_{MDEA} : mass fraction of MDEA
$w_{[N1111][Gly]}$: mass fraction of [N1111][Gly]
$[C_8mim][Tf_2N]$: 1-octyl-3-methylimidazolium Bis (trifluoromethyl) Sulfonylimide
$[Bmin][MeSO_4]$: 1-butyl-3-methylimidazolium methylsulfate
$[Bmim][PF_6]$: 1-butyl-3-methylimidazolium hexafluorophosphate
$[C_2min][eFAP]$: 1-ethyl-3-methylimidazolium tris (pentafluoroethyl) Trifluorophosphate
[MDEAH][Ac] : methyldiethanolammonium acetate
[MDEAH][For] : methyldiethanolammonium formate
[DMEAH][Ac] : dimethylethanolammonium acetate
[DMEAH][For] : dimethylethanolammonium formate

REFERENCES

1. China business intelligence network https://s.askci.com/data/MonthDetail/Index?zbId=a03010f&type=2&isYear=1&StartTime=&EndTime=&CityCode=, 2021 (accessed 18 July 2021).
2. J. K. Park, S. Y. Lee, J. I. Kim, W. Um and C. Yoo, *J. Environ. Chem. Eng.*, **9**, 105037 (2021).
3. G. P. Wang, *China Metallurgy*, **22**, 25 (2012).
4. L. de Oliveira Carneiro, S. F. de Vasconcelos, G. W. de Farias Neto, R. P. Brito and K. D. Brito, *Sep. Purif. Technol.*, **257**, 117862 (2021).
5. H. Yan and J. S. Tian, *Fuel Chem. Process.*, **35**, 25 (2004).
6. L. A. Kazak, A. F. Yarmoshik and V. M Li, *Coke Chem.*, **61**, 376 (2018).
7. C. Q. Yan and L. R. Yu, *Fuel. Chem. Process.*, **35**, 26 (2004).
8. P. Huang and K. C. Ling, *Coal Convers.*, **28**, 64 (2005).
9. L. J. Zhang, *Metallurgical Power*, **3**, 17 (2013).
10. P. Nasir and A. E. Mather, *Can. J. Chem. Eng.*, **55**, 715 (1977).
11. C. F. Song, Q. L. Liu, N. Ji, S. Deng, J. Zhao and Y. Kitamura, *Appl. Energ.*, **204**, 353 (2017).
12. F. Anu, Y. A. Rikov, G. L. Kuranov and N. A. Smirnova, *Russ. J. Appl. Chem.*, **80**, 515 (2007).
13. M. H. Li and K. P. Shen, *J. Chem. Eng. Data*, **38**, 105 (1993).
14. J. R. An, P. F. Ma, J. F. Tang, X. Jiang, J. Li, G. J. Zhang and M. Y. Zhao, *Chem. Ind. Eng. Prog.*, **35**, 3866 (2016).
15. D. A. Glasscock and G. T. Rochelle, *AIChE J.*, **39**, 1389 (1993).
16. B. P. Mandal, A. Biswas and S. Bandyopadhyay, *Sep. Purif. Technol.*, **35**, 191 (2004).
17. M. Li, S. Zhang, P. Zhang, K. Qin, B. Xu, J. Zhou, C. Yuan, Q. Cao and H. Xiao, *Chem. Eng. J.*, **436**, 135251 (2022).
18. A. Haghtalab and A. Afsharpour, *Fluid Phase Equilib.*, **406**, 10 (2015).
19. D. W. Savage, E. W. Funk, W. C. Yu and G. Astarita, *Ind. Eng. Chem. Fundamen.*, **25**, 326 (1986).
20. A. Kazemi, M. Malayeri, A. G. Kharaji and A. Shariati, *J. Nat. Gas Sci. Eng.*, **20**, 16 (2014).
21. R. K. Abdulrahman and I. M. Sebastine, *J. Nat. Gas Sci. Eng.*, **14**, 116 (2013).
22. X. F. Tian, L. M. Wang, D. Fu and C. Li, *Energy Fuel*, **33**, 629 (2019).
23. X. F. Tian, L. M. Wang and D. Fu, *Energy Fuel*, **33**, 8413 (2019).
24. X. F. Tian, L. M. Wang, P. Zhang, D. Fu and Z. Y. Wang, *Environ. Sci. Pollut. R.*, **28**, 5822 (2021).
25. R. Sidi-Boumedine, S. Horstmann, K. Fischer, E. Provost, W. Fürst and J. Gmehling, *Fluid Phase Equilib.*, **218**, 149 (2004).
26. M. E. Rebolledo-Libreros and A. Trejo, *Fluid Phase Equilib.*, **224**, 83 (2004).
27. J. Z. Xia, A. Kamps and G. Maurer, *Fluid Phase Equilib.*, **207**, 23 (2003).
28. D. Speyer, A. Böttger and G. Maurer, *Ind. Eng. Chem. Res.*, **51**, 12549 (2012).
29. Z. Q. Bi and L. S. Shen, *Anhui Metallurgy*, **2**, 29 (2008).
30. B. Y. Zhang and D. X. Jin, *Sci. Technol. Baotou Steel Co.*, **2**, 4 (2001).
31. Z. Cai, Y. Ma, J. Zhang, W. Wu, Y. Cao, L. Jiang and K. Huang, *Fuel*, **313**, 122664 (2022).
32. Y. Cao, J. Zhang, Y. Ma, W. Wu, K. Huang and L. Jiang, *ACS Sustain. Chem. Eng.*, **9**, 7352 (2021).
33. R. Giernoth, *Angew. Chem. Int. Ed.*, **49**, 2834 (2010).
34. M. Damanafshan, B. Mokhtarani, M. Mirzaei, M. Mafi, A. Sharifi and A. H. Jalili, *J. Chem. Eng. Data*, **63** 2135 (2018).
35. A. Barati-Harooni, A. Najafi-Marghmaleki and A. H. Mohammadi, *Int. J. Greenh. Gas Con.*, **63**, 338 (2017).
36. K. Huang, X. M. Zhang, L. S. Zhou, D. J. Tao and J. P. Fan, *Chem. Eng. Sci.*, **173**, 253 (2017).
37. F. Liu, W. Chen, J. Mi, J. Y. Zhang, X. Kan, F. Y. Zhong, K. Huang, A. M. Zheng and L. Jiang, *AIChE J.*, **65**, e16574 (2019).
38. M. Nematpour, A. H. Jalili, C. Ghotbi and D. Rashtchian, *J. Nat. Gas Sci. Eng.*, **30**, 583 (2016).
39. L. Y. Wang, Y. L. Xu, Z. D. Li, Y. N. Wei and J. P. Wei, *Energy Fuel*, **32**, 10 (2017).
40. B. Seyedhosseini, M. Izadyar and M. R. Housaindokht, *J. Phys. Chem. A.*, **121**, 4352 (2017).
41. D. Fu, P. Zhang and C. L. Mi, *Energy*, **101**, 288 (2016).
42. D. Fu and J. L. Xie, *J. Chem. Thermodyn.*, **102**, 310 (2016).
43. Z. M. Zhou, G. H. Jing and L. J. Zhou, *Chem. Eng. J.*, **204**, 235 (2012).
44. S. Aparicio and M. Atilhan, *Energy Fuel*, **24**, 4989 (2015).
45. W. Y. Lee, S. Y. Park, K. B. Lee and S. C. Nam, *Energy Fuel*, **34**, 1992 (2020).
46. J. G. Lu, Y. F. Zheng and D. L. He, *Sep. Purif. Technol.*, **52**, 209 (2006).
47. A. H. Jalili, M. Safavi, C. Ghotbi, A. Mehdizadeh, M. Hosseini-Jenab and V. Taghikhani,. *J. Phys. Chem. B.*, **116**, 2758 (2012).
48. A. H. Jalili, M. Shokouhi, G. Maurer and M. Hosseini-Jenab, *J. Chem. Thermodyn.*, **67**, 55 (2013).
49. M. B. Shiflett, A. M. S. Niehaus and A. Yokozeki,. *J. Chem. Eng. Data*, **55**, 4785 (2010).
50. K. Huang, X. M. Zhang, Y. Xu, Y. T. Wu, X. B. Hu and Y. Xu, *AIChE J.*, **60**, 4232 (2014).
51. M. B. Shiflett and A. Yokozeki, *Fluid Phase Equilib.*, **294**, 105 (2010).